Grabemann, I.; Groll, N.; Moeller, J.; Weisse, R.:

Climate change impact on North Sea wave conditions:
A consistent analysis of ten projections

In: Ocean Dynamics (2014) Springer

DOI: 10.1007/s10236-014-0800-z

Climate change impact on North Sea wave conditions: a consistent analysis of ten projections

Iris Grabemann[1], Nikolaus Groll[1], Jens Möller[2] and Ralf Weisse[1]

[1] Institute for Coastal Research, Helmholtz-Zentrum Geesthacht Centre for Materials and Coastal Research, Max-Planck-Str. 1, 21502 Geesthacht, Germany

[2] Bundesamt für Seeschifffahrt und Hydrographie, Bernhard-Nocht-Str. 78, 20359 Hamburg, Germany

Reference: Ocean Dynamics (2015) 65:255–267 DOI 10.1007/s10236-014-0800-z
Link: http://link.springer.com/article/10.1007/s10236-014-0800-z

Abstract

Long-term changes in the mean and extreme wind wave conditions as they may occur in the course of anthropogenic climate change can influence and endanger human coastal and offshore activities. A set of ten wave climate projections derived from time slice and transient simulations of future conditions is analyzed to estimate the possible impact of anthropogenic climate change on mean and extreme wave conditions in the North Sea. This set includes different combinations of IPCC SRES emission scenarios (A2, B2, A1B and B1), global and regional models and initial states. A consistent approach is used to provide a more robust assessment of expected changes and uncertainties.

While the spatial patterns and the magnitude of the climate change signals vary, some robust features among the ten projections emerge: mean and severe wave heights tend to increase in the eastern parts of the North Sea towards the end of the twenty-first century in nine to ten projections, but the magnitude of the increase in extreme waves varies in the order of decimeters between these projections. For the western parts of the North Sea more than half of the projections suggest a decrease in mean and extreme wave heights. Comparing the different sources of uncertainties due to models, scenarios and initial conditions it can be inferred that the influence of the emission scenario on the climate change signal seems to be less important. Furthermore, the transient projections show strong multi-decadal fluctuations, and changes towards the end of the twenty-first century might partly be associated with internal variability rather than with systematic changes.

1 Introduction

Wind-generated waves at the ocean surface vary substantially in response to atmospheric forcing. The mean and extreme wave climates are essential for many coastal and offshore operations. Examples comprise, among others, coastal and offshore shipping, coastal protection, or operation and design of offshore wind farms or oil and gas platforms. Long-term changes in wave climate have therefore received considerable attention, either historically (e.g. Kushnir at al, 1997; Gulev and Grigorieva, 2004; Sterl and Caires, 2005; Weisse and Günther, 2007) or as potential future developments in the course of anthropogenic climate change (e.g. Caires et al, 2006; Mori et al, 2010; Dobrynin et al, 2012; Semedo et al, 2013; Wang et al, 2014).

Studies focusing on the aspects of potential future anthropogenic changes in wave climate are mainly driven by regional interests and many of the existing studies nowadays concentrate on specific regions (e.g. Debernard and Røed (2008) or de Winter et al (2012) for the North Sea, Brown et al (2011) for parts of the Irish Sea, Lionello et al (2008) for the Mediterranean, Andrade et al (2007) for the Portuguese coast or Hemer et al (2010) for the southeast coast of Australia, among others). Global wave climate projections based on dynamical approaches have only recently become available (e.g. Mori et al (2010), Hemer et al (2012a), Fan et al (2013), Semedo et al (2013), comparative study by Hemer et al (2013)). The advantage of the latter is that they enable inter-comparability between different regions, potentially helping in identifying hotspots of changes or regions of risk (as discussed in COWCLIP, see Hemer et al (2012b)) and in identifying large-scale patterns and causes of change. The computational efforts in producing such global projections are enormous, their number and spatial resolution will likely remain limited in the near future.

Regional projections will remain a valuable tool for detailed assessments also in the near future. Downscaling approaches for regional projections are computationally also still demanding such that the number of cases considered remains comparably small (typically in the order of one up to four, e.g. Andrade et al (2007), Debernard and Røed (2008)) and assessment of uncertainty ranges remains limited. The latter is, however, needed when robust adaptation measures should be developed which efficiently work under a broad range of future wave climate conditions.

Future anthropogenic changes in the wave climate of the North Sea based on dynamical downscaling have been studied, for example, by Debernard and Røed (2008), Grabemann and Weisse (2008), Lowe et al (2009), de Winter et al (2012) or Groll et al (2014a). Within these studies, considerable variation in the projected wave climate seems to occur. Whereas the pattern seems to be somewhat similar with a tendency to an increase of severe wave heights in eastern and southern parts of the North Sea and with a tendency to a decrease in western and northern parts, the magnitude of such changes varies strongly between the projections. Such variations may arise from different atmospheric forcing derived from different climate models forced with different greenhouse gas emission scenarios as well as from using different analysis techniques (e.g. different percentiles or return values for different periods: long-term, annual, winter, etc). While variations due to different atmospheric forcing represent the uncertainty in wave climate projections, variations caused by different analysis techniques hamper the comparability of the different studies.

In this study, a consistent analysis and systematic comparison of ten future projections of North Sea wave conditions is presented in order to provide a more robust figure of expected changes by determining common changes and to investigate contributions of different atmospheric forcing to the uncertainty of possible future changes in North Sea wave climate.

These ten projections describe an *ensemble of opportunity*; such an ensemble is characterized by non-scientific aspects such as availability of data which determine the size and composition of such ensembles and for which the sampling is neither random nor systematic (Tebaldi and Knutti, 2007). Ensembles of opportunity encompass variations between ensemble members that are not

Table 1: Set of ten wave climate simulations. The six projections based on the scenarios A1B and B1 differ in their underlying RCMs and in the initial conditions (IC) of the underlying simulations for the global climate and the four projections based on the scenarios A2 and B2 differ in their underlying GCMs. The simulation identifiers consists of two to three letters before the underscore presenting the reference simulations (C20) or the future climate projections described by the respective scenario (e.g. A1B). The one to two letters after the underscore present the initial condition (1, 2 or 3) and the RCM (C, R or H) in case of the six transient projections or the GCM (E or H) in case of the four time slice projections.

identifier	WAM version	RCM providing meteorological output for WAM	GCM providing output for RCM		IPCC scenario	time span
C20_1C	4.5.3	COSMO-CLM	ECHAM5/MPI-OM	IC1		1961-2000
A1B_1C		(Rockel et al. 2008)	(Röckner et al. 2003)		A1B	2001-2100
B1_1C			(Marsland et al. 2003)		B1	2001-2100
C20_2C	4.5.3	COSMO-CLM	ECHAM5/MPI-OM	IC2		1961-2000
A1B_2C					A1B	2001-2100
B1_2C					B1	2001-2100
C20_3R	4.5.3	REMO	ECHAM5/MPI-OM	IC3		1961-2000
A1B_3R		(Jacob et al. 2007)			A1B	2001-2100
C20_3H	4.5.3	HIRHAM	ECHAM5/MPI-OM	IC3		1961-2000
A1B_3H		(Christensen et al. 2007)			A1B	2001-2100
C20_E	4.5	RCAO	ECHAM4/OPYC3			1961-1990
A2_E		(Rummukainen et al. 2001)	(Röckner et al. 1999)		A2	2071-2100
B2_E		(Räisänen et al. 2004)			B2	2071-2100
C20_H	4.5	RCAO	HadAM3H			1961-1990
A2_H			(Gordon et al. 2000)		A2	2071-2100
B2_H					B2	2071-2100

just caused by natural internal variability in the climate system, but also from model and forcing scenario differences (von Storch and Zwiers, 2012). The latter is problematic when formulating and testing hypotheses in a statistical sense (von Storch and Zwiers, 2012). However, caused by the enormous computational effort in generating the individual members, such ensembles of opportunity presently represent the state-of-the-art and status quo in climate modelling. We therefore follow the discussion in von Storch and Zwiers (2012) and provide a simple descriptive approach for characterizing the information in our ensemble of projections acknowledging the effect that results may change in a different ensemble even if our understanding of the climate system remains unchanged (Tebaldi and Knutti, 2007).

2 Models, ensemble setup and statistical analysis

The ensemble of opportunity for the North Sea (Figure 2) studied here includes ten already existing future projections of the wave climate (Table 1 and Figure 2) in which the simulations of the ocean wind waves were driven with regionalized atmospheric data from simulations of the global climate. For the underlying simulations of the global and regional climate, different emission scenarios, initial conditions and general (global) circulation (GCMs) and regional climate (RCMs) models are incorporated (Table 1). In the following, this ensemble and the models in-

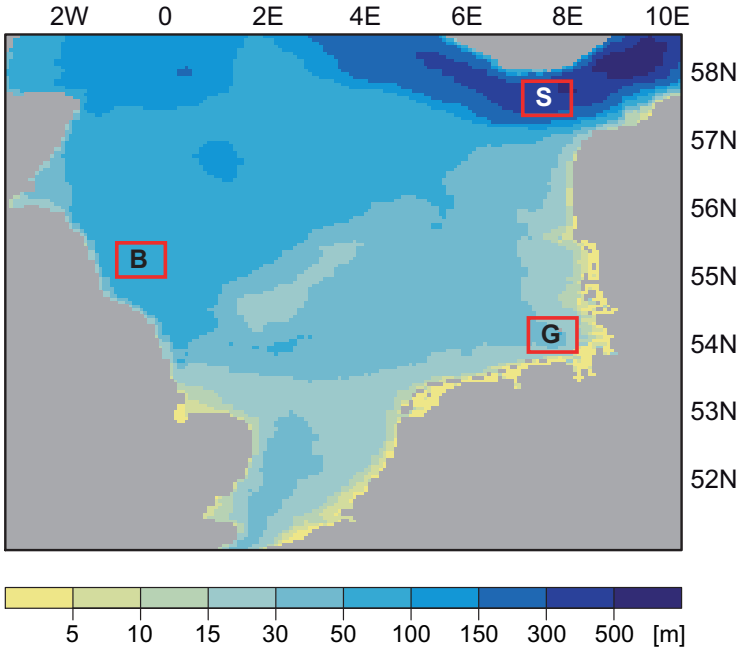

Figure 1: Model domain and bathymetry in meters for the fine North Sea grid of the wave model WAM (version 4.5.3). Area B (British coast) is located at 0.85°W-0.05°E, 54.9-55.35°N, area G (German Bight) at 7.25-8.15°E, 54-54.35°N and area S (off the Skagerrak) at 7.25-8.15°E, 57.30-57.75°N.

volved are described shortly; more detailed information can be found in Grabemann and Weisse (2008) and Groll et al (2014a,b).

2.1 The wave model WAM

The ocean wind waves in the ten projections were simulated using two versions (4.5 and 4.5.3) of the third generation spectral wave model WAM (WAMDI-Group, 1988). This state-of-the-art wave model has been validated and used in several studies which show that the model is capable of reproducing the North Sea wave climate at a reasonable degree of accuracy (e.g. Weisse and Günther, 2007).
In all cases a nested approach was used. The coarse grid has a horizontal resolution of 0.5° x 0.75° (latitude x longitude) which corresponds roughly to a 50 km x 50 km grid. The grid covers parts of the North East Atlantic to take into account swell generated outside and propagating into the North Sea. Sea ice conditions from corresponding simulations of the global climate are used. The fine grid has a resolution of about 5.5 km x 5.5 km (0.05° x 0.1° and 0.05° x 0.075° for longitude x latitude in version 4.5 and 4.5.3, respectively). It covers the North Sea from 51°S to 58.5°N and 3.25°W to 10.25°E. The fine grid simulations get the spectral wave information at the boundaries from the coarse grid simulations. The wave spectra for both grids (coarse and fine) are calculated for 25 frequencies (version 4.5.3) and for 28 frequencies (version 4.5), respectively, and 24 directions. The model is used in shallow water mode with depth refraction. The integration time step is one minute and wave parameters are stored every hour. The output of the wave model is used to calculate mean and extreme wave height statistics.

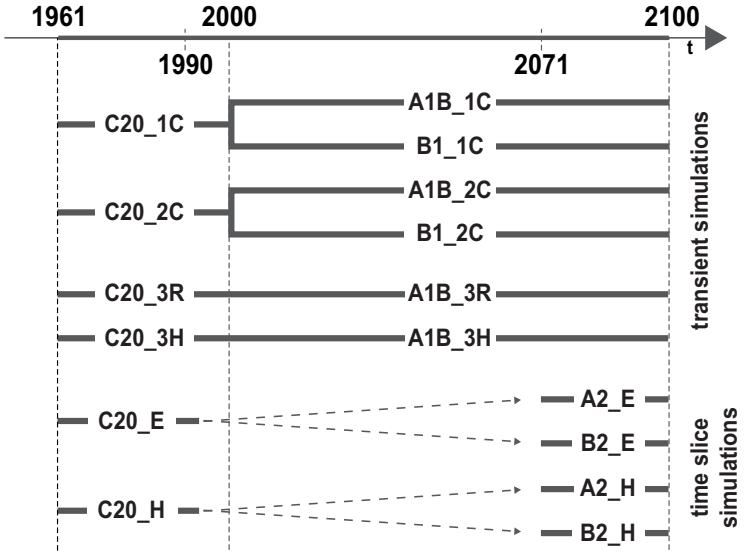

Figure 2: Ensemble setup and time period under consideration. The labels give the identifiers as defined in Table 1.

2.2 Ensemble of opportunity

To estimate the future range of possible changes in North Sea wave conditions an ensemble of ten simulations was used. The driving atmospheric models, initial conditions and scenarios are listed in Table 1 together with the identifiers for the reference and projected wave climates. A schematic illustration of the reference and projection periods is summarized in Figure 2.

This ensemble of opportunity consists of six 140-year long projections based on one coupled atmosphere-ocean GCM, two emission scenarios and three different initializations accounting for internal natural variability. The three different initializations origin from randomly chosen dates derived from long quasi-equilibrium simulations with fixed external forcings (for more details see Hollweg et al (2008)). From 1860 to 2000 these three simulation are forced by observed greenhouse gas concentrations. Subsequently, from 2001 to 2100 the simulations are forced with the two IPCC SRES emission scenarios A1B and B1 (Houghton et al, 2001; Nakicenovic and Swart, 2000). The global simulations were subsequently dynamically downscaled from 1960 onwards using three different RCMs.

Furthermore, the ensemble consists of four 30-year long projections for the IPCC SRES scenarios A2 and B2 (Houghton et al, 2001; Nakicenovic and Swart, 2000) which differ in their underlying two GCMs. Simulations for the reference climates and the climate projections were done for 1961-1990 and 2071-2100, respectively, and were regionalized with one RCM.

The RCM simulations were used to generate four 40-year-long (1961-2000) and two 30-year-long (1961-1990) wave simulations for the 20th century and corresponding six 100-year-long (2001-2100) and four 30-year-long (2071-2100) wave simulations under climate change scenario conditions, respectively, with the model WAM (see Figure 2 und Table 1).

Together with their respective reference climate simulations the A1B and B1 projections and the A2 and B2 projections are referred to as *transient* and *time slice* simulations, respectively (see Figure 2).

The different 20th century reference simulations (C20) were validated against measurements and data from a hindcast (Weisse and Günther, 2007) which was driven by NCAR-NCEP reanalyses atmospheric data. For a more detailed description of the different reference climates and their validations as well as the future climate projections: for the time slice projections A2_E,

A2_H, B2_E and B2_H see Grabemann and Weisse (2008), for the transient projections A1B_1C, A1B_2C, B1_1C and B1_2C see Groll et al (2014a) and for the two transient projections A1B_3H and A1B_3R see Groll et al (2014b).

2.3 Statistical analysis

Changes in the significant wave height (SWH) as obtained from the ten projections are consistently analysed and presented as follows.
For each of the ten projections, the annual 50th (median) and the annual 99th percentile and the annual maximum SWH were calculated from the hourly values for every grid point in the model domain of the fine North Sea grid. The annual median, the annual 99th percentile and the annual maximum SWH were averaged over the 30-year time slices 1961-1990 and 2071-2100 in case of the reference climates and climate projections. The *climate change signal* at every grid point is defined as the difference between the 30-year mean of the annual 50th, 99th percentile or maximum SWH of a climate projection and the respective 30-year mean of its reference climate for 1961-1990.
Independent of its magnitude, the climate change signal is either positive or negative describing either an increase or a decrease of the significant wave height for 2071-2100 relative to 1961-1990. To identify common changes, at each grid point the number of projections N sharing the same sign of change was determined rather than calculating ensemble means (see von Storch and Zwiers (2012) for discussion on this issue). As the time slice and the transient simulations were performed on different model grids (see section 2.1), the data were interpolated on the least common grid (0.3^o x 0.15^o) for comparison. To give additionally the range of the projected changes in wave conditions, climate change signals are also analysed for each projection.
This range of the projected changes may arise from different atmospheric forcing which results from the different emission scenarios, GCMs, RCMs or initial states included in the 10 projections. To test the similarity of the climate change signals in the ten projections with respect to the different forcing factors a combined analysis of pattern correlation and mean absolute difference was introduced to those projections which differ only by two factors.
For three selected areas with an extent of 0.9^o x 0.45^o near different coasts of the North Sea (see Figure 2) area-averaged time series were extracted. For these areas box plots of the annual median, annual 99 percentile and annual maximum SWH were calculated for the year 1961-1990 and 2071-2100 to investigate changes in the main distribution parameters. In order to compare the simulated variability in the reference and projection periods with the natural variability, the respective distribution parameters based on area-averaged annual median, annual 99th percentile and annual maximum SWH were extracted from the 50-year long aforementioned hindcast (Weisse and Günther, 2007). As the model domain of the hindcast simulation is limited to 56^oN, such values can be shown for area B and G only. In order to be consistent with the boxplot analysis, here the *natural variability* is defined as the 25th and 75th percentiles of annual values from the hindcast.
To elaborate the temporal variability of the climate change signal over the 140 years from 1961 to 2100, time series of the 30-year-running means for the area-averaged annual median, annual 99th percentile and annual maximum SWH at the three selected areas were used. The 30-year running means are again presented relative to the reference climate 1961-1990. To display the variability within the 30-year running periods, 25th and 75th percentiles were calculated from the 30 annual values and were compared to the natural variability derived from the hindcast.

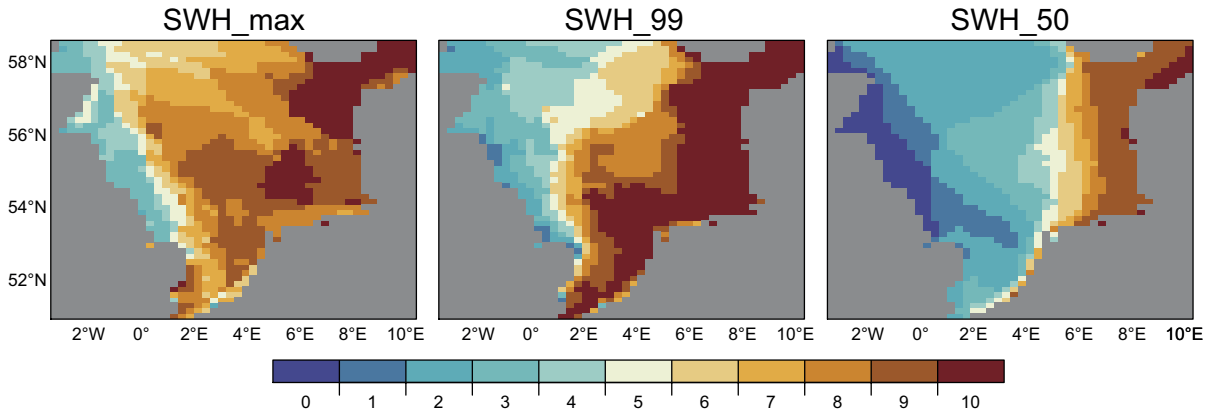

Figure 3: Spatial distributions of the number of projections N for which the climate change signals of the 30-year mean of the annual maximum (SWH_max, left), 99th percentile (SWH_99, middle) and median SWH (SWH_50, right) for 2071-2100 relative to 1961-1990 have a positive sign.

3 Results

3.1 Climate change signals for 2071-2100

In the following, common features and differences in the climate change signals obtained from the ten projections are elaborated for the whole model domain of the North Sea for the end of the twenty-first century (2071-2100). Such common features for all 10 projections arise from the spatial distribution of the number of projections N for which the climate change signals have the same sign. A common change is defined as *robust* if at least nine projections have the same sign.

The climate change signals of the annual maximum SWH (Figure 3, left) show an increase for more than half of the projections in most areas in the North Sea. For parts of the southern North Sea and toward the eastern coasts and the Skargerrak, nine to ten projections have the same sign showing an robust increase. Along parts off the British coast, more than half of the projections show a decrease in maximum SWH but this change is less robust.

The climate change signals of the annual 99th percentile SWH (Figure 3, middle) display an increase in the southern and eastern North Sea in most of the projections. For the areas off the Dutch, German and Danish coasts, nine to ten projections agree in an increase in 99th percentile SWH covering similar areas as for the maximum SWH. In the northwestern parts, more than half of the projections reveal a negative but less robust change.

In case of the annual median SWH (Figure 3, right), the spatial pattern presents an east-west directed increase in the number of projections with a positive sign of the climate change signal. In the most eastern North Sea, an increase in median SWH is dominant and can be seen in at least nine projections. Toward the British coast of the North Sea, nine to ten projections show a robust decrease of the median SWH.

Figure 3 displays whether an increase or a decrease in SWH is dominant in the ten projections without giving the magnitude of this increase or decrease. In the following, the range of this magnitude as obtained from the ten projections is displayed. Figure 4 presents the climate change signals for the annual maximum SWH for each of the ten projections. The projections A2_E and B2_E show an overall positive climate change signal, only very small areas in the western North Sea show a negative signal. The projections A2_H and B2_H show generally the smallest changes. The largest changes occur in the Skargerrak and south of the Norwegian coast in the projections A1B_1C, A1B_3R and A1B_3H. There the climate change signals vary from a few centimeters to

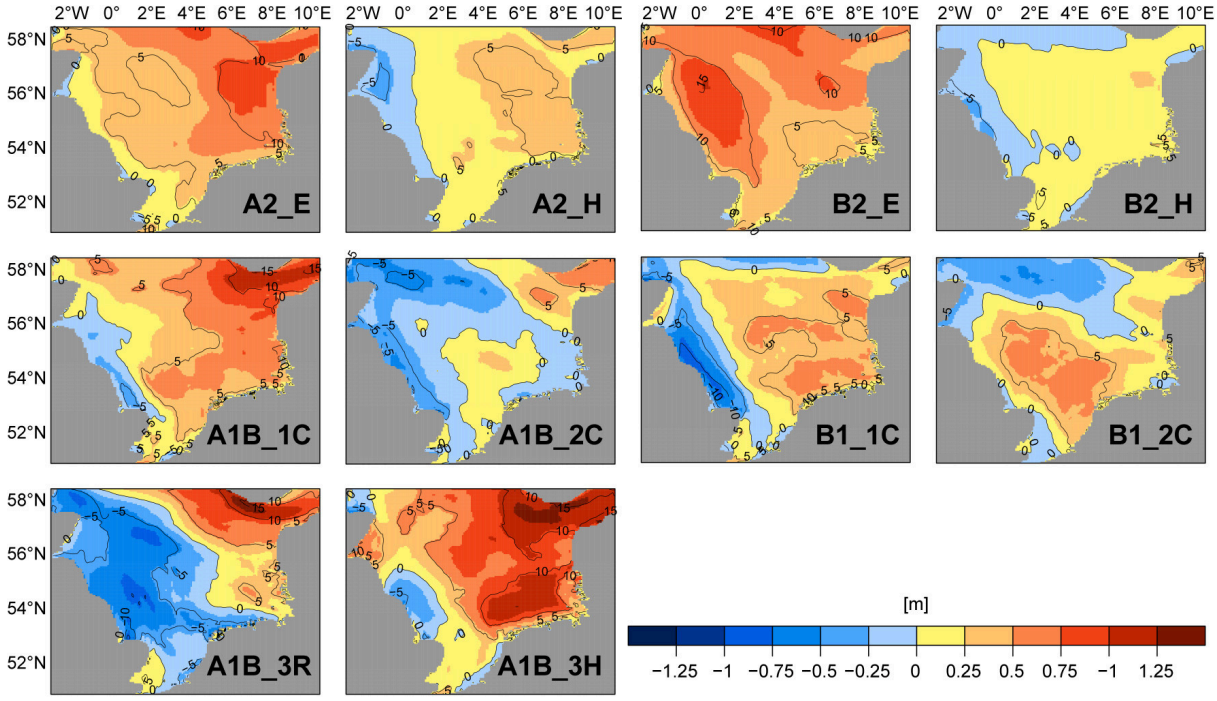

Figure 4: Spatial distributions of the climate change signals of the 30-year mean of annual maximum SWH in meters for the period 2071-2100 relative to 1961-1990 for each of the 10 projections. Contour lines present changes in % of the reference wave conditions.

more than 1.25 m. In the German Bight, the increase in mean annual maximum SWH range up to about 1 m (A1B_3H), but one projection shows a decrease (A1B_2C). Off the northern British coast where projections with a negative climate change signal dominate, a decrease up to about -75 cm occurs in A1B_3R. There, the largest positive signal for maximum wave conditions reach up to about 75 cm in B2_E. The smallest variability between the climate change signals of the ten projections occurs north of the English channel with signals ranging between about -25 cm and about 25 cm. Summarizing, over the entire North Sea area and between the ten projections, the range of the climate change signal is about -10 % to 15 % relative to the reference SWH. The relative changes of the annual median and 99th percentile SWH (not shown) are in the same order of magnitude as the relative changes of the annual maximum, but the spatial distributions of the changes are different (see for examples Grabemann and Weisse (2008); Groll et al (2014a)).
To display the contributions of the different forcing factors (like scenarios, GCMs, RCMs, initial states) to the detected future changes in wave conditions, Figure 5 presents a comparison of the climate change signals between different projection combinations which is based on pattern correlation and mean difference. The comparison is limited to combinations of projections which differ only in two forcing factors.
The simulations which differ in their two forcing GCMs and two emission scenarios are shown by rhombs in Figure 5. For the climate change signals of the annual median and the 99th percentile SWH, the combinations A2_E/B2_E and A2_H/B2_H (green rhombs, same GCM but different emission scenarios) are more similar with correlation coefficients exceeding 0.9 and relatively small mean differences than the combinations A2_E/A2_H and B2_E/B2_H (blue rhombs, same scenario but different GCMs) or the combinations A2_E/B2_H and B2_E/A2_H (black rhombs). This points out that the underlying GCMs seem to have more influence than the chosen emission scenarios in these combinations. This result is less obvious for the climate change signals of the annual maximum SWH.
The simulations with the same GCM but with different initial conditions and emission scenarios

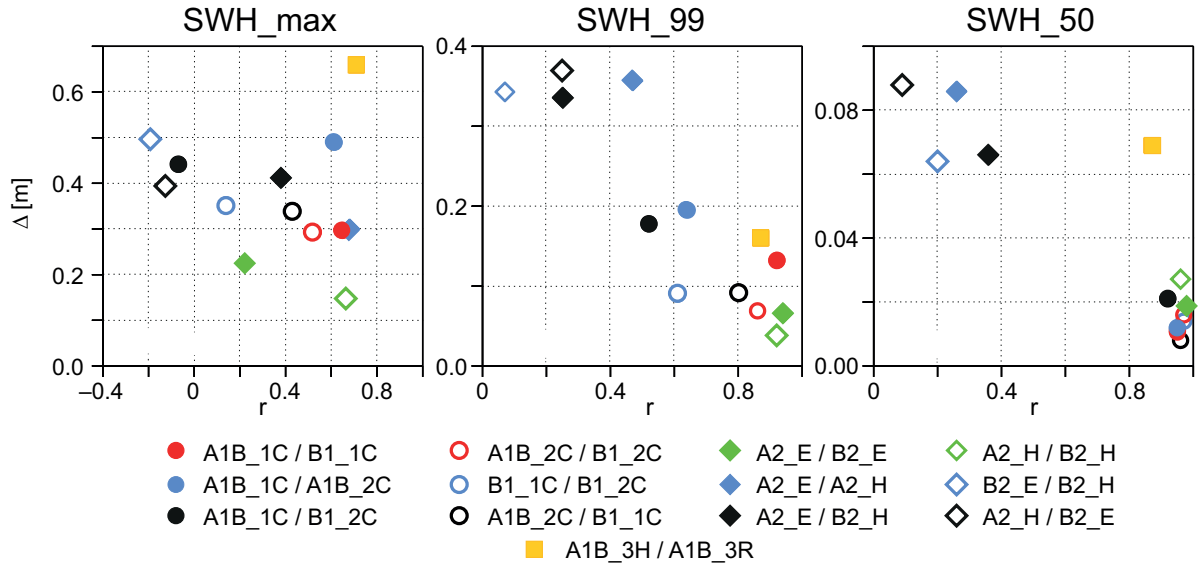

Figure 5: Comparison of the climate change signals of the annual maximum (SWH_max, left), 99th percentile (SWH_99, middle) and median SWH (SWH_50, right) for 2071-2100 for 13 pairs of two projections. The x-axis displays the pattern correlation coefficient r and the y-axis the mean absolute difference Δ in meters between two projections in each case. Pairs of A1B_1C, B1_1C, A1B_2C and B1_2C (different initial conditions and scenarios) are presented by dots, pairs of A2_E, B2_E, A2_H and B2_H (different GCMs and scenarios) are shown by rhombs. The yellow square displays the pair A1B_3R/A1B_3H (different RCMs.)

are displayed by circles in Figure 5. For the annual median SWH, all combinations show high correlation coefficients of more than 0.9 and relative small mean differences. Thus, a differentiation for a larger influence of the initial conditions or the scenarios on the climate change signals is not possible. For the annual 99th percentile and maximum SWH, the effect of the initial condition on the climate change signal seems to be more or similar important as the effect of the emission scenario. The combinations A1B_1C/B1_1C and A1B_2C/B1_2C (red circles, same initial conditions but different scenarios) show higher (less) or comparable pattern correlations (mean differences) compared to the combinations A1B_1C/A1B_2C and B1_1C/B1_2C (blue circles, same scenario but different initial conditions) or A1B_1C/B1_2C and A1B_2C/B1_1C (black circles).
The comparison of the climate change signals for the projections A1B_3H and A1B_3R (yellow square, same emission scenario, GCM and initial condition but different RCMs) shows the importance of the chosen RCM. The pattern correlation coefficient is comparable to other combinations, but the mean difference is comparably high. Thus, whereas the patterns are relatively similar, the amplitudes of the climate change signals depend on the chosen RCM.

3.2 Distributions of annual SWH parameters at three areas

In the following, the distributions of the annual values of the individual 30 years for each projection 2071-2100 and the respective reference climate 1961-1990 are displayed for the three selected areas by boxplots (Figure 6). The means of each box for the projections correspond to the climate change signals at the specific areas in Figure 4.
For areas G and S, the differences between the mean of the 30 annual maximum SWH of each climate projection and the mean of the respective reference climate are positive for at least nine or all ten projections. The same is valid for the annual median and the annual 99th percentile

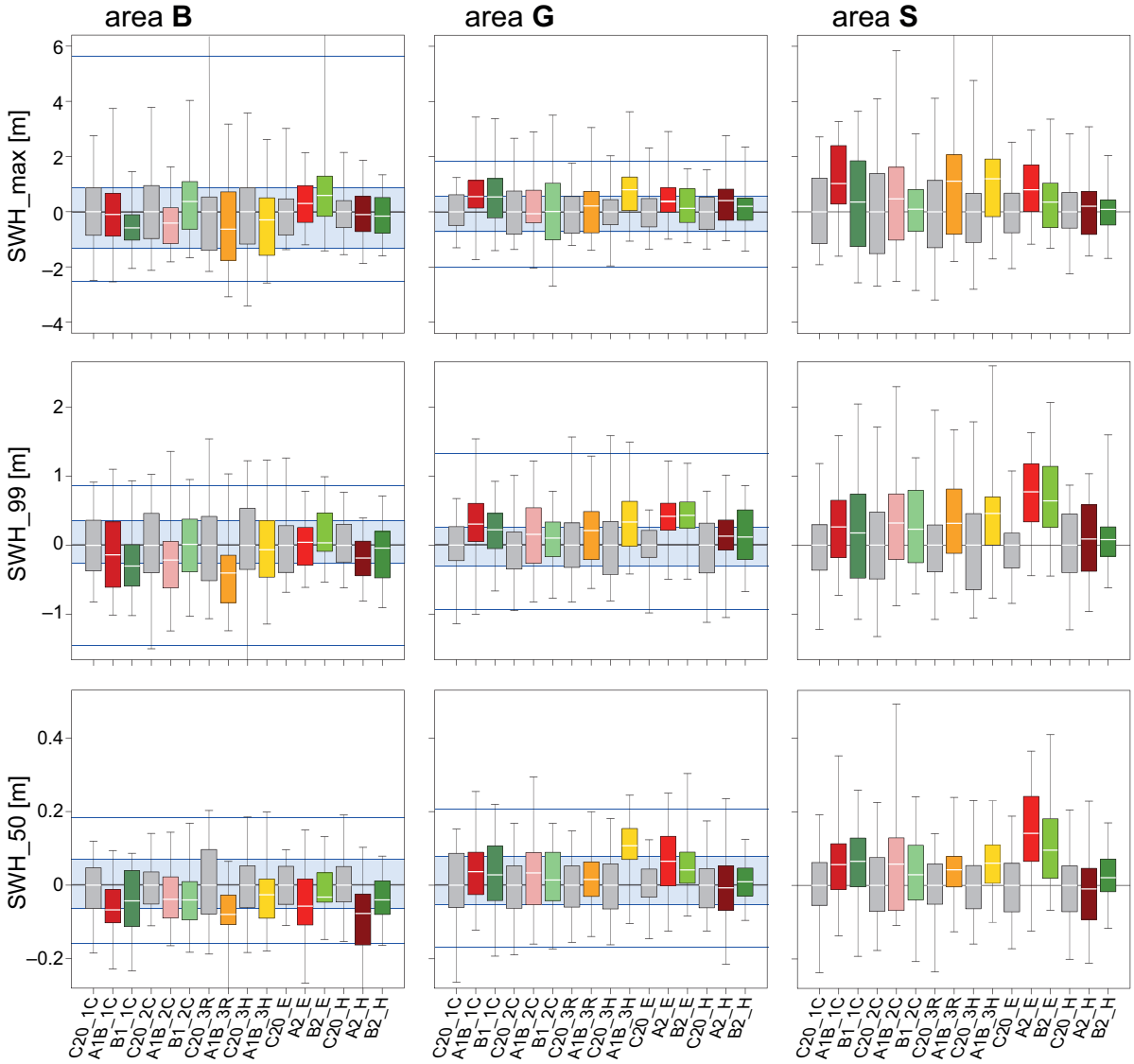

Figure 6: Boxplots of area-averaged annual maxima (SWH_max, top), 99th percentile (SWH_99, middle) and median SWH (SWH_50, bottom) in meters for the 10 projections for 2071-2100 and the respective reference climates for 1961-1990 for the three selected areas displayed in Figure 2. The boxes are plotted relative to the mean of the respective reference climate. They present the 25th to the 75th percentiles and the vertical bars show the minimum and the maximum of the annual values. Grey shaded boxes represent the reference climates, the colored boxes display the climate projections. The four blue horizontal lines for the areas B and G depict the maximum, 75th and 25th percentiles and minimum SWH of the respective annual values from the 50-year long hindcast for 1958 to 2007 described in Weisse and Günther (2007).

(Figure 6). For area B, the differences are negative for seven projections in case of the annual maximum and 99th percentile, and they are negative for all projections in case of the median SWH (Figure 6). These findings are in accordance with those given in Figures 3 and 4.
In the reference climate, 50 % (between the 25th and 75th percentile) of the annual maxima represented by the boxes vary up to about 2 m (areas B and G) or 3 m (area S). For all three areas, the boxes are overlapping for most of the projections and their respective reference climate which point to non-robust changes within each single projection. There is no general

tendency for a widening or narrowing of the distribution in the ten projections. Similar results are generally obtained for the annual median and 99 percentile SWH with a few exceptions. For areas B and G, the variability in the reference simulations is similar to or slightly smaller than the natural variability as displayed by the 50-year long hindcast showing that most of the reference simulations represent the natural variability.

3.3 Multi-decadal variability at three areas

Figure 7 presents time series of the 30-year running means of the area-averaged annual maximum SWH together with the respective running 25th and 75th percentiles (see section 2.3) for the three locations for the six transient projections.
To show that the climate simulations are capable to simulate a realistic variability of 30-year running means of the area-averaged annual maximum SWH in the reference period, they are compared to those derived from the aforementioned hindcast for areas B and G (red lines in Figure 7). At area B no trend is evident in the hindcast and at the beginning of the six climate simulations. At area G an almost linear increase of the 30-year running mean annual maxima can be seen in the hindcast and in half of the climate simulations. Thus the variability at the beginning of the simulations is within the variability derived from the hindcast for these two areas.
At all three areas, the transient projections show multi-decadal variability within each projection and considerable scatter between the six projections. Between all projections throughout the simulation period, these multi-decadal variations are between about -60 cm and 1.4 m for the area off the Skagerrak (area S), between about -30 cm and 1 m for the area in the German Bight (area G) and between about -80 cm and 60 cm for the area off the British coast (area B). Therefore, the multi-decadal variability of the climate change signals is in the order of -10% to 15% of the reference conditions.
Superimposed there appears to be a small tendency of the 30-year running mean of the annual maximum SWH to an increase toward 2100 at the areas G and S and a small tendency to a decrease at area B. The changes for 2071-2100 (area G: -10 to 80 cm, area S: 10 to 125 cm, area B: -60 to 40 cm) are in agreement with the findings shown at the specific locations in Figures 3 and 4 and with the changes shown by the boxplots in Figure 6 for the single projections.
A variability of the annual values within the running 30-year periods (displayed in grey by the running 25th and 75th percentiles) is seen at all three areas. For area B, the 30-year running means of the annual maximum SWH are within the natural variability given by the aforementioned hindcast (displayed in blue by the 25th and 75th percentiles of the 50 annual maxima). The projected variability is also in most time periods within the range of the natural variability. For area G, the 30-year running means of the annual maximum SWH exceed in the projections A1B_1C and B1_1C in a few time periods and in the projection A1B_3H in most time periods the natural variability. But also in these time periods the variability of the 30 annual maxima is still overlapping with the natural variability.
Time series of the 30-year running means of the area-averaged annual median and 99th percentile significant wave heights (not shown) at the same locations display comparable multi-decadal fluctuations. These findings are in agreement with those for the 30-year running means of the median and 99 percentile SWH shown for other areas in Groll et al (2014a) for four of these six projections.
Independent of the area, these time series for the climate change signals of the area-averaged annual median, 99th percentile and maximum SWH point out that the multi-decadal fluctuations are in the same order of magnitude as the change (increase or decrease) toward 2071-2100.

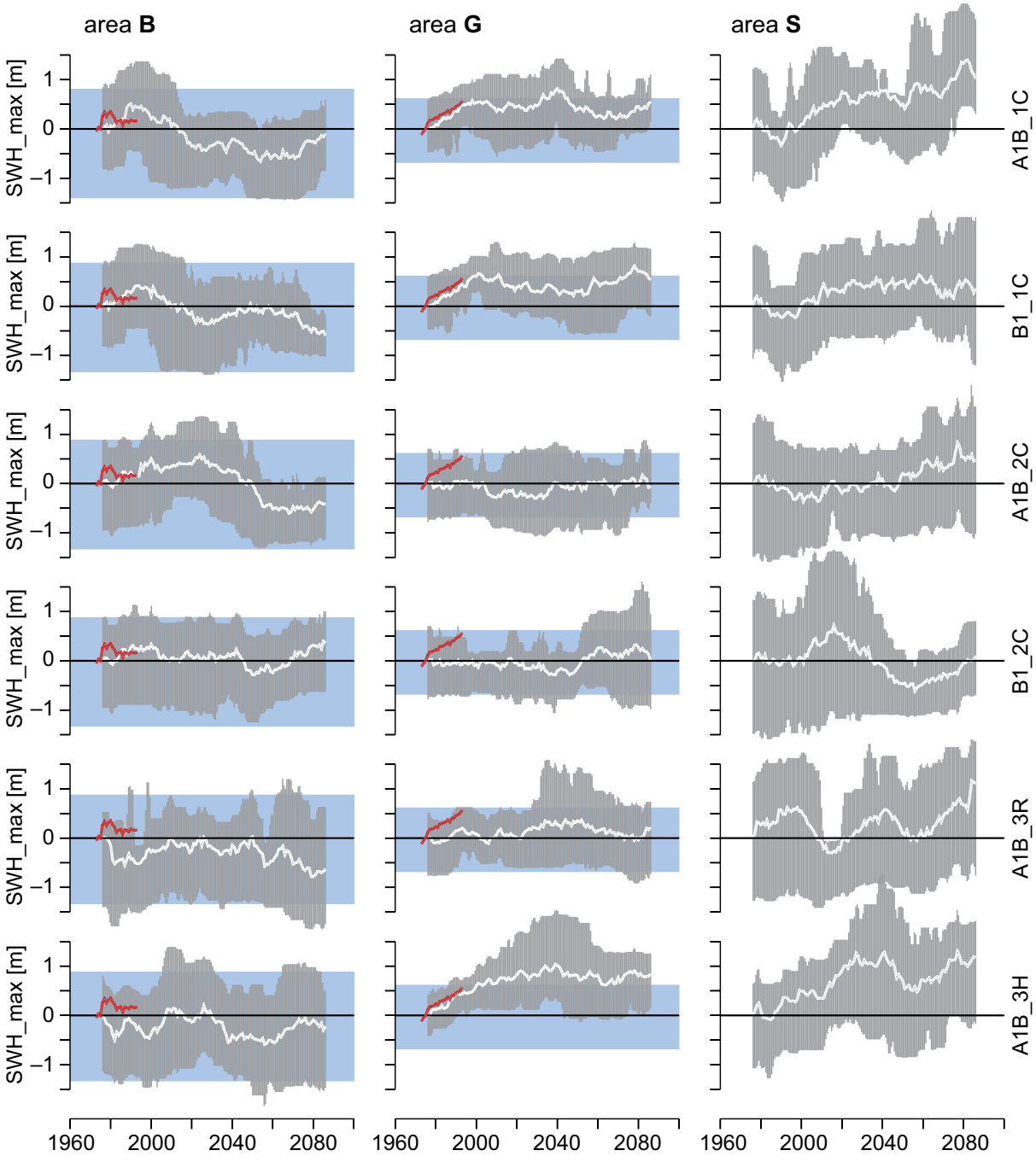

Figure 7: 30-year running means of the area-averaged annual maximum SWH in meters for the three chosen areas displayed in Figure 2 relative to the corresponding mean for the period 1961-1990 for the six transient projections. Grey shadings present the variability given by the 25th and 75th percentiles of the area-averaged 30 annual values for each of the running 30-year time slices. The blue shadings and the red lines display the respective 25th and 75th percentiles (representing the natural variability) and the area-averaged 30-year running means, respectively, as derived from annual values of the 50-year long hindcast (Weisse and Günther, 2007).

4 Discussion and Conclusions

The ten projections of possible future wave conditions studied here are based on different emission scenarios and on different global and regional models starting from different initial conditions. Each emission scenario is equally consistent and plausible and basically reflects different assumptions on future socioeconomic development. All underlying models represent the state-of-the-art and projections from different models are thus considered equally likely.
These ten projections were consistently analyzed and systematically compared to detect differences and similarities in the projected changes in SWH and to provide robust patterns of expected changes and uncertainty ranges. Two main conclusions can be drawn.

1. The increase in SWH for the annual maximum, 99th percentile and median for 2071-2100 compared to 1961-1990 in the eastern parts of the North Sea is a robust feature among the ten projections considered.

2. There is multi-decadal variability apparent in the transient projections that is in the same order of magnitude as potential changes towards the end of the twenty-first century. Moreover, the projected variability seldom exceeds the natural variability defined here by the 25th and 75 percentiles of annual maximum, 99th percentile and median SWHs from a hindcast.

Nine to ten projections agree in an increase of the SWH for the annual maximum, 99th percentile and median for 2071-2100 compared to 1961-1990 in the eastern North Sea. The spatial distribution of the robust change is relatively similar for the maximum and the 99th percentile SWH. It covers parts of the southeastern North Sea and large parts off the Dutch, German and Danish coasts up to the Skagerrak. For the median the spatial distribution of the robust change is smaller und restricted to the most east. For some parts off the British coast, nine to ten projections show a robust decrease in case of median climate change signals. However, the aforementioned robust changes in all domains are smaller than 5 % relative to the reference climate. Larger changes are found in single projections but not consistently in nine to ten members.
Whereas the sign of change appears to be a robust feature in some areas of the North Sea, the magnitude of possible future changes in mean and severe SWH is much more uncertain. For the three distribution parameters, climate change signals between the projections vary between about -10 % and 15 % relative to the reference SWH.
Debernard and Røed (2008) investigated a set of four climate projections including combinations of three emission scenarios (A1, A1B and B2) and three different GCMs. The climate change signals for 2071-2100 in comparison with 1961-1990 vary in their spatial pattern and in their magnitude between the four projections. Overall, severe SWHs (99 percentiles) agree in an increase along the east coast of the North Sea and the Skagerrak (6-8 % for a combined analysis) whereas a decrease occurs to the west and/or north of the North Sea. Lowe et al (2009) compared the time periods 2070-2100 and 1960-1990 for emission scenario A1B, they found changes in the mean annual maximum SWH between -1.5 m and 1 m. Changes with a negative sign occur along the North Sea coast of Great Britain and in the northern North Sea and those with a positive sign in the southern and eastern North Sea. de Winter et al (2012) investigated means of a 17 member ensemble for the emission scenario A1B based on one GCM. The comparison of the time periods 2071-2100 and 1961-1990 shows that the mean SWHs remain unaltered in front of the Dutch coast for the selected locations. There, changes in annual maximum SWHs vary around zero (about -0.1 to 0.1 m). For a few selected locations in the central to the northern North Sea, changes in annual maximum SWH have a negative sign (about -0.5 to -0.2 m). Changes in these studies are in the same order of magnitude as the changes derived from the ten future climate projections presented in this study.

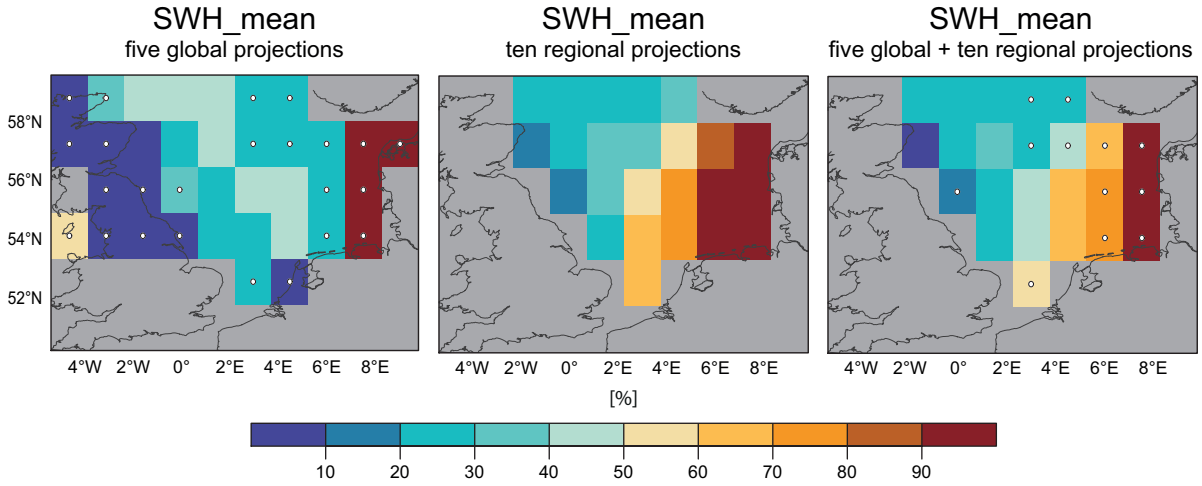

Figure 8: Spatial distribution of the number N of projections (in % of the number of available projections per grid point) for which the climate change signals of the long-term mean SWH have a positive sign using the five global simulations (left), the ten regional projections (interpolated to the global grid, middle) and the five global and ten regional projections (right). Due to the different global land-sea-masks, there are grid points with less than the five considered global projections, these grid points are marked by circles. The five global projections used for this comparison originates from Mori et al (2010), Hemer et al (2012b) (two projections), Fan et al (2013) and Semedo et al (2013).

In order to put the results from the ten regional projections presented here into a broader perspective, they are compared to those from recently available global wave projections (Hemer et al (2013), available at https://wiki.csiro.au/display/sealevel/COWCLIP+Contributions). Using dynamically downscaled projections, this comparison is limited to five CMIP3 wave simulations which are originally described in Mori et al (2010), Hemer et al (2012b) (two projections), Fan et al (2013) and Semedo et al (2013). Three of the five individual climate change signals of the global wave projections suggest a tendency to an increase of the mean SWH toward the eastern coasts up to +10% and all five signals tend to decrease toward the Northwest up to approximately -10%. These changes are in the same order of magnitude as those given by the ten regional projections for medium conditions. However, the coarse resolution and the use of different land-sea-masks in these global projections hamper the comparison. These global projections agree with the common change of the regional projections in a common decrease in the Northwest of the North Sea (Figure 8), whereas a common increase in the eastern North Sea is hardly to identify. The common change signal of the five global and ten regional projections displays also an increase (decrease) of the mean SWH in the eastern (western) North Sea in the majority of the projections. To keep the focus on the dynamical projections, the global statistical projections (Wang and Swail (2006), available at https://wiki.csiro.au/display/sealevel/COWCLIP+Contributions) are not included in the analysis of the common change shown in Figure 8. However, incorporating these statistical projections to the common change (not shown) the general pattern would not change.

In the course of the twenty-first century, the transient regional projections display variations of the climate change signals on multi-decadal time scales and the strongest signals (increase or decrease) do not necessarily occur toward the end of the century. Throughout the simulation period 2001-2100, the climate change signals for the three distribution parameter (annual median, 99th percentile and maximum SWH) vary for the three areas and between all projections between about -10 % and about 15 % relative to the reference conditions. These variations which

are superimposed on the long-term changes indicate the internal variability and are in the same order of magnitude as the increase or decrease toward the end of the century.
At the three selected areas, the distributions of the annual median, 99th percentile and maximum SWH show no general trend towards a widening or a narrowing within the ten regional projections for 2071-2100 relative to 1961-1990 or within the six transient projections for which the distributions (given by the 25th and 75th percentiles) vary over the consecutive 30-year time periods. Grabemann and Weisse (2008) and Groll et al (2014a) suggested that the increase in median and 99th percentile SWH toward 2100 for the eastern North Sea mainly result from an increase in frequency of higher waves.
The tendency to an increase of the median and severe SWHs in the eastern/southern parts and the tendency to a decrease in the western/northern parts of the North Sea is in accordance with changes in the driving wind fields. Strong winds from westerly directions become more frequent toward 2100 and waves propagate more often toward the east (Grabemann and Weisse, 2008; Groll et al, 2014a). Changes to more frequent stronger westerly winds toward the end of the twenty-first century is also projected in studies of, e.g., Debernard and Røed (2008) and de Winter et al (2012). de Winter et al (2013) present similar findings for the North Sea in global CMIP5 projections. For the transient projections A1B and B1 wind velocity and direction also show multi-decadal variations (Gaslikova et al, 2013; Groll et al, 2014a,b). For the A1B and B1 projections used here, Pinto et al (2007) noted for the underlying GCM simulations that a shift to more strong westerly winds is in accordance with a shift towards more positive North Atlantic oscillation (NAO) phases. Additionally they showed multi-decadal variability of the NAO-index throughout the twenty-first century.
Concerning the sources of uncertainties in the ten regional wave climate projections for 2071–2100, it was found in case of the four projections A2_E, B2_E, A2_H and B2_H that for the median and the 99 percentile SWH the model-based differences are larger than the emission scenario-induced differences. A similar conclusion is presented by Debernard and Røed (2008) for a slightly different set of four projections using the scenarios A2 and B2. Wang and Swail (2006) also concluded that the uncertainty due to differences caused by different GCMs is greater than that due to differences among the emission scenarios. Comparing the projections A1B_1C, A1B_2C, B1_1C and B1_2C, the effect of the initial condition seems to be stronger as or similar to the effect of the emission scenario for the 99th percentile SWH. For the median SWH these projections are comparably similar. Furthermore, the differences in the projections A1B_3R and A1B_3H reflect the importance of the RCM in estimating the climate change signals. Such impacts due to GCMs, RCMs, initial conditions and emission scenarios is less obvious in the maximum SWH. Summarizing, the differences in the climate change signals due to the used GCMs, RCMs, initial conditions and emission scenarios in the ten projections suggest that the choice of the emission scenario has less influence on the simulated future wave climate than the other three components at least for medium and 99th percentile SWHs. Additionally, the multi-decadal variations in the transient projections, point to an uncertainty from the choice of the selected time period.
For the regional ensemble presented here, it is important to note that apart from using four different RCMs, four emission scenarios and three different initial conditions, only two different GCMs are included. This could lead to a biased interpretation of the ten regional projections. Using a larger set of GCMs in regional projections could lead to a more generalized ensemble by incorporating different large scale atmospheric circulation variability (e.g. NAO) and should be taken into account in future regional ensemble studies of the wave climate.
Summarizing, the results shown here together with those from other studies indicate that the increase in median and severe SWH in the eastern North Sea towards the end of the twenty-first century appears to be a robust feature. The magnitude of this increase is much more uncertain. In the western North Sea, projections with a decrease in SWH dominates, but this signal is

less robust for severe SWH. Within the twenty-first century, the climate change signals for the SWH vary on multi-decadal time scales. These variations point to the internal climate variability and are in the same order of magnitude as the climate change signals toward the end of the twenty-first century.

Acknowledgements
The authors are thankful to A. Behrens for assistance with theWAM model and to B. Gardeike for assistance with the graphics. This investigation was partly supported in the context of the joint project AKÜST (Changes in the coastal climate – evaluation of alternative strategies in coastal protection, Förderkennzeichen VWZN2455, Az. 99-22/07) and in the context of the Governmental Research Programme KLIWAS (Impacts of Climate Change on Waterways and Navigation – Development of Adaptation Options).

References

Andrade C, Pires HO, Taborda R, Freitas MC (2007) Projecting future changes in wave climate and coastal response in Portugal by the end of the 21st century. J Coast Res 50:257–263

Brown J, Wolf J, Souza AJ (2011) Past to future extreme events in Liverpool Bay: model projections from 1960-2100. Climatic Change 111:365–391, DOI 10.1007/s10584-011-0145-2

Caires S, Swail V, Wang X (2006) Projection and analysis of extreme wave climate. J Climate 19:5581–5605, DOI 10.1175/JCLI3918.1

Christensen OB, Drews M, Christensen JH, Dethloff K, Ketelsen KM, Hebestadt I, Rinke A (2007) The HIRHAM Regional Climate Model Version 5 (beta). Technical Report 06-17, 22pp, Danish Meteorological Institute

Debernard J, Røed L (2008) Future wind, wave and storm surge climate in the Northern Seas: a revisit. TELLUS A 60(3):427–438, DOI 10.1111/j.1600-0870.2008.00312.x

Dobrynin, Murawsky, Yang (2012) Evolution of the global wind wave climate in CMIP5 experiments. Geophysical Research Letters 39:18, DOI 10.1029/2012GL052843

Fan Y, Held IM, Lin S, Wang XL (2013) Ocean warming effect on surfave gravity wave climate change for the end of the twenty-first century. J Climate 26, 6046–6066, DOI 10.1175/JCLI-D-12-00410.1

Gordon C, Cooper C, Senior CA, Banks H, Gregory JM, Jones TC, Mitchell JFB, Wood RA (2000) The simulation of SST, sea ice extents and ocean heat transports in a version of the Hadley Centre coupled model without flux adjustments. Clim Dyn 16:147-166

Gaslikova L, Grabemann I, Groll N (2013) Changes in North Sea storm surge conditions for four transient future climate realizations. Nat Hazards, DOI 10.1007/s11069-012-0279-1

Grabemann I, Weisse R (2008) Climate change impact on extreme wave conditions in the north sea: an ensemble study. Ocean Dynamics 58:199–212, DOI 10.1007/s10236-008-0141-x

Groll N, Grabemann I, Gaslikova L (2014a) North Sea wave conditions: an analysis of four transient future climate realizations. Ocean Dynamics 64:1–12, DOI 10.1007/s10236-013-0666-5

Groll N, Weisse R, Behrens A, Günther H, Möller J (2014b) Berechnung von Seegangsszenarien für die Nordsee. Bundesanstalt für Gewässerkunde - KLIWAS Koordination (Hrsg.), Koblenz, Germany, DOI 10.5675/Kliwas_64/2014_Seegangsszenarien

Gulev S, Grigorieva 4 (2004) Last century changes in ocean wind wave height from global visual wave data. Geophys Res Lett 31(L24601), DOI 10.1029/2004GL021032

Hemer MA, Church JA, Hunter JR (2010) Variability and trends in the directional wave climate of the Southern Hemispere. International Journal of Climatology 30(4):475–491

Hemer MA, Katzfey J, Trenham C (2012a) Global dynamical projections of surface ocean wave climate for a future high greenhouse gas emssion scenario. Ocean Modeling 70,221–245, DOI 10.1016/j.ocemod.2012.09.008

Hemer MA, Wang XL, Weisse R, Swail VR (2012b) Advancing Wind-Waves Climate Science The COWCLIP Project. Bull Am Met Soc 93:791–796, DOI 10.1175/BAMS-D-11-00184.1

Hemer MA, Fan Y, Mori N, Semedo A, Wang XL (2013) Projected changes in wave climate from a multi-model ensemble. Nature Climate Change 3:471–476, DOI 10.1038/NCLIMATE1791

Hollweg H, Böhm U, Fast I, Hennemuth B, Keuler K, Keup-Thiel E, Lautenschlager M, Legutke S, Radtke K, Rockel B, Schubert M, Will A, Woldt M, Wunram C (2008) Ensemble simulations over Europe with the regional climate model CLM forced with IPCC AR4 global scenarios. Technical report 3, Support for Climate- and Earth System Research at the Max Planck Institute for Meteorology, ISSN 1619-2257

Houghton J, Ding Y, Griggs D, Noguer M, van der Linden P, Dai X, Maskell K, Johnson C (eds) (2001) Climate Change 2001: The Scientific Basis. Contribution of Working Group I to the Third Assessment Report of the Intergovernmental Panel on Climate Change. Cambridge University Press, United Kingdom and New York

Jacob D, Bähring L, Christensen OB, Christensen JH, Castro de M, Déqué Mn Giorgi F, Hagemann S, Hirschi M, Jones R, Kjellströrm R,Lenderink G, Rockel B, Sánchez E, Schär C, Senevirate S, Sornot S, Ulden van A, Hurk van den B (2007) An intercomparison of regional climate models for Europe: Design of the experiments and model performance. Climatic Change 81, Supplement 1:31–52

Kushnir Y, Cardone V, Greenwood J, Cane M (1997) The recent increase in North Atlantic wave heights. J Clim 10:2107–2113

Lionello P, Cogo S, Galatin MB, Sanna A (2008) The Mediterranean surface wave climate inferred from future scenario simulations. Global and Planetary Change 63(203): 152–162

Lowe JA, Howard TP, Pardaens A, Tinker J, Holt J, Wakelin S, Milne G, Leake J, ans K Horsburgh JW, Reeder T, Jenkins G, Ridley J, Dye S, Bradley S (2009) UK Climate Projections science report: Marine and coastal projections. Met Office Hadley Centre, Exeter, UK, ISBN 978-1-906360-03-0

Marsland S, Haak H, Jungclaus J, Latif M, Röske F (2003) The Max-Planck-Institute global ocean/sea ice model with orthogonal curvilinear coordinates. Ocean Modeling 5:91–127

Mori N, Yasuda T, Mase H, Tom T, Oku Y (2010) Projections of extreme wave climate change under global warming. Hydrol Res Lett 4:15–19

Nakicenovic N, Swart R (eds) (2000) Special Report of the Intergovernmental Panel on Climate Change on Emission Scenarios. Cambridge University Press, United Kingdom, [Summary available online at http://www.ipcc.ch/pub/reports.htm]

Pinto J, Ulbrich U, Leckebusch G, Spangehl T, Reyers M, Zacharis S (2007) Changes in the storm track and cyclone activity in the three SRES ensemble experiments with the ECHAM5/MPI-OM1 GCM. Clim Dyn 29:195–210, doi:10.1007/s00,382–007–0230–4

Räisänen J, Hansson U, Ullerstig A, Döscher R, Graham LP, Jones C, Meier HEM, Samuelsson P and Willén U (2004) European climate in the late twenty-first century: regional simulations with two driving global models and two forcing scenarios. Clim Dyn 22:13–31, DOI 10.1007/s00382-003-0365-x

Rockel B, Will A, Hense A (eds) (2008) Special issue Regional climate modeling with COSMO-CLM (CCLM), vol 17. Met. Zeitschrift

Röckner E, Bengtsson L, Feichter J, Lelieveld J, Rodhe H (1999) Transient climate change simulations with a coupled atmosphere-ocean GCM including the trophospheric sulfer cycle. J Climate 12:3004–3032

Röckner E, Bäuml G, Bonaventura L, Brokopf R, Esch M, Giorgetta M, Hagemann, Kirchner I, Kornblueh L, Manzini E, Rhodin A, Schlese U, Schulzweida U, Tompkins A (2003) The atmospheric general circulation model echam5. part i: model description. Mpi - rep 349, Max Planck Institute for Meteorology

Rummukainen M, Räisänen J, Bringfelt B, Ullerstig A, Omstedt A, Willén U Hansson U, Jones C (2004) A regional climate model for Northern Europe: model description and results from the downscaling of two GCM control simulations. Clim Dyn 17:339–359

Semedo A, Weisse R, Behrens A, Sterl A, Bengtsson L, Günther H (2013) Projection of global wave climate change toward the end of the twenty-first century. J Climate 26:8269–8288

Sterl A, Caires S (2005) Climatology, variability and extremes of ocean waves -The web-based KNMI/ERA-40 wave atlas. Int J Climatol:963–977, DOI 10.1002/joc.1175

Storch von H, Zwiers F (2012) Testing ensembles of climate change scenarios for "statistical significance". Climatic Change 17:1–9, DOI 10.1007/s10584-012-0551-0

Tebaldi C, Knutti (2007) The use of the multi-model ensemble in probabilistic climate projections. Philos Trans R Soc A 365:2053–2075, DOI 10.1098/rsta.2007.2076

WAMDI-Group (1988) The wam model – a third generation ocean wave prediction model. J Phys Oceanogr 18:1776–1810

Wang XL, Swail V (2006) Climate change signal and uncertainty in projections of ocean wave heights. Ocean Dynamics 26: 109–126, DOI 10.1007/s00382-005-0080-x

Wang XL, Feng, Swail V (2014) Changes in global ocean wave heights as projected using multimodel CMIP5 simulations. GRL: 109–126, DOI 10.1002/2013GL058650

Weisse R, Günther H (2007) Wave climate and long-term changes for the southern north sea obtained from a high-resolution hindcast 1958 – 2002. Ocean Dynamics 57:161–172, DOI 10.1007/s10236-006-0094-x

Winter de RC, Sterl A, de Vries JW, Weber SL, Ruessink G (2012) The effect of climate change on extreme waves in front of the dutch coast. Ocean Dynamics 62:1139–1152, DOI 10.1007/s10236-012-0551-7

Winter de RC, Sterl A, Ruessink G (2013) Wind extremes in the North Sea Basin under climate change: an ensemble study of 12 CMIP5 GCMs. J Geophys Res Atmos 118:1601–1612, DOI 10.1002/jgrd.50147